

Electronic Supplementary Information (ESI)

1. Experimental section

1.1 Materials

The chemicals were purchased from Sinopharm Chemical Reagent Co., Ltd.. All chemicals were used as received without further purification.

1.2 Pre-treatment of the Fe wires

The Fe wires with diameter of 1mm were first washed by acetone to remove the oil contaminants on the surface by sonicating for 5 min. After dried in air, a following sonication in 0.1 M HCl solution (10 min) was conducted to remove the surface oxides.

1.3 Preparation of the solution for bluing treatment (Solution A)

36 g NaOH and 14 g NaNO₂ were dissolved in 50 mL H₂O under vigorous stirring, and a transparent solution was formed as the the solution for bluing treatment (Solution A).

1.4 Synthesis of B-NiCoFe, B-Fe and B-Fe/B-NiCo

A piece of cleaned Fe wire and certain amounts of Ni(NO₃)₂·6H₂O and Co(NO₃)₂·6H₂O with a total concentration of 0.2 mol/L were placed into a beaker with 50 mL boiling Solution A with temperature of approximately 165 °C, and a piece of glass-surface vessel was covered on the beaker. After reacting for 3 min, the Fe wire becomes black, and the as-obtained product was washed by deionized water and ethanol, respectively and dried under vacuum. By varying the ratio of Ni/Co salt precursors, the B-NiCoFe catalysts with Co:Ni ratio of 2:1, 1:1 and 1:2 can be prepared. Besides, B-Fe catalyst can be obtained in the same condition with the absence of Ni/Co salts. In addition, a two-step procedure was involved in the synthesis of B-Fe/B-NiCo, in which a bluing Fe wire (B-Fe) was used instead of the bare Fe wire as the substrate.

1.5 Synthesis of HT-NiCoFe

A piece of cleaned Fe wire was added into 40 mL deionized water containing 1.164g $\text{Ni}(\text{NO}_3)_2 \cdot 6\text{H}_2\text{O}$, 1.164g $\text{Co}(\text{NO}_3)_2 \cdot 6\text{H}_2\text{O}$, 28.8g NaOH and 11.2g NaNO_2 , and the reaction system was transferred into a 50 mL Teflon-lined stainless-steel autoclave. Then, the autoclave was sealed and maintained at 165 °C for 10h, and then allowed to cool to room temperature naturally. The as-obtained product was washed by deionized water and ethanol, respectively and dried under vacuum.

1.6 Structural characterizations

The X-ray diffraction (XRD) was performed on a Philips X'Pert Pro Super diffractometer with Cu $K\alpha$ radiation ($\lambda=1.54178 \text{ \AA}$). The scanning electron microscopy (SEM) images were taken on a JEOL JSM-6700F SEM. The transmission electron microscopy (TEM) was carried out on a JEM-2100F field emission electron microscope at an acceleration voltage of 200 kV. The high-resolution TEM (HRTEM) was performed on a JEOL-2010 transmission electron microscope at an acceleration voltage of 200 kV. A Perkin Elmer Optima 7300DV ICP emission spectroscope was used for the inductively coupled plasma optical emission spectrometry (ICP-OES) analyses to identify the concentration of Ni, Co and Fe, and the concentrations of the metals are calculated as the molar percentage in the total amount of metal. The X-ray photoelectron spectroscopy (XPS) analyses were performed on a VGESCALAB MKII X-ray photoelectron spectrometer with an excitation source of Mg $K\alpha = 1253.6 \text{ eV}$, and the resolution level was lower than 1 atom%.

1.7 Experimental details on the OER performance

All the electrochemical measurements were performed in a three-electrode system linked with an electrochemical workstation (CHI660E) at room temperature. All potentials were calibrated to a reversible hydrogen electrode (RHE) and the data are presented without iR correction. The cyclic voltammetry (CV) and linear sweep voltammetry (LSV) with a scan rate of 5 mV s^{-1} were conducted in O_2 -purged 1 M KOH solution. A Hg/HgO electrode was used as the reference electrode, a platinum gauze electrode ($2 \text{ cm} \times 2 \text{ cm}$, 60 mesh) was used as the counter electrode, and the Fe

wire based catalysts were served as the working electrodes which were connected directly to the electrochemical workstation. The electrochemical impedance spectroscopy (EIS) measurements were operated at variable potentials from 10^{-2} - 10^5 Hz, and the CV cycling tests for stability evaluation were performed at a scan rate of 50 mV s^{-1} .

2. Supplementary physical characterizations

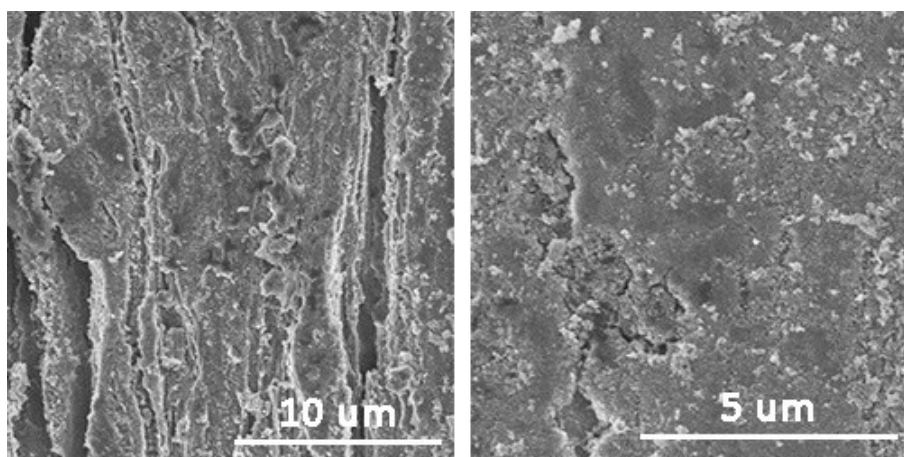


Fig. S1 SEM images of the B-Fe/B-NiCo.

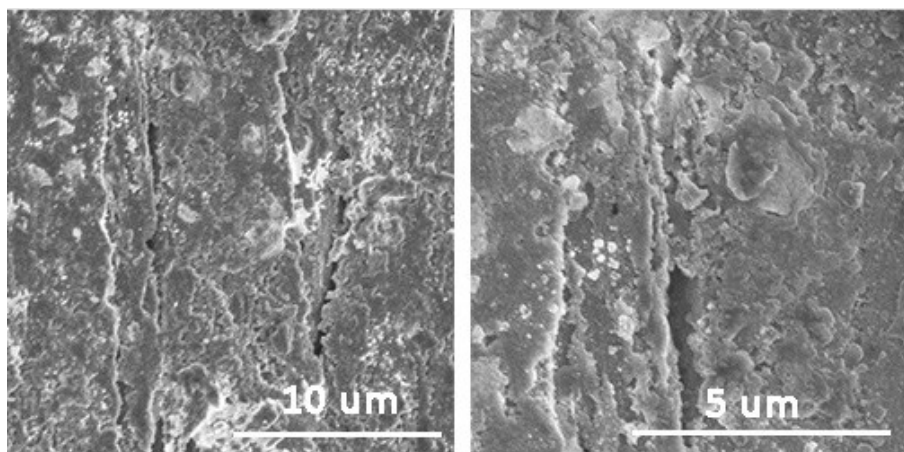


Fig. S2 SEM images of the B-Fe.

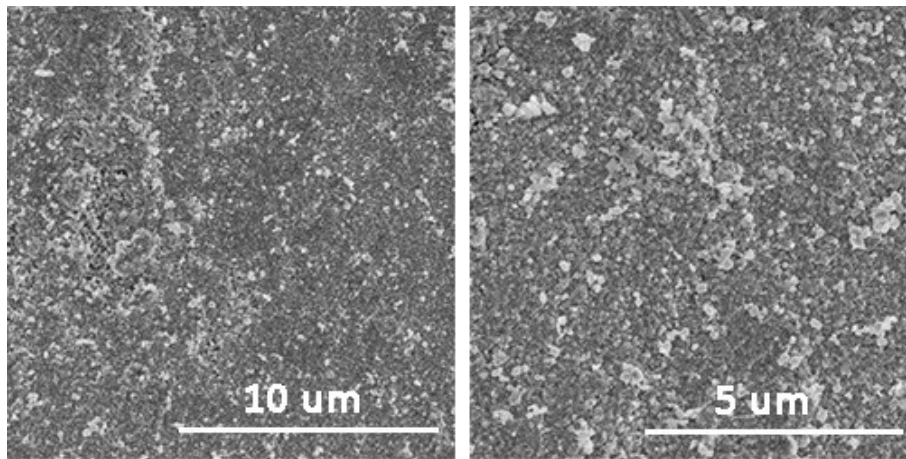


Fig. S3 SEM images of the HT-NiCoFe.

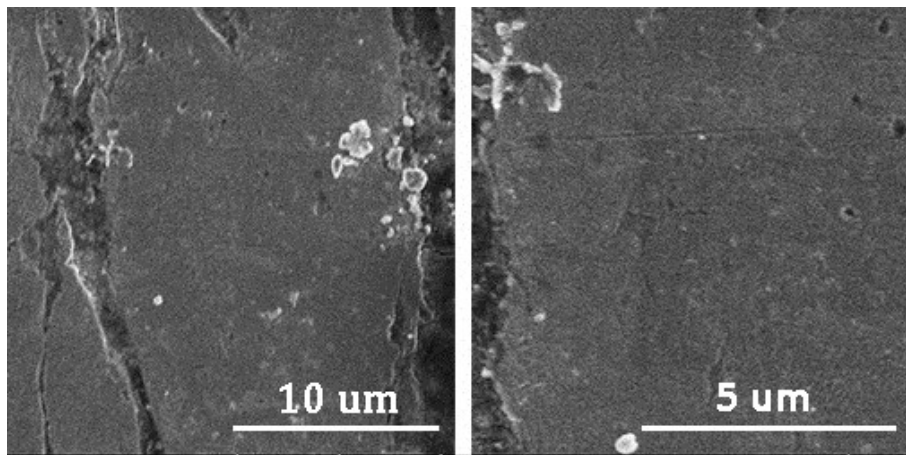


Fig. S4 SEM images of the bare Fe wire.

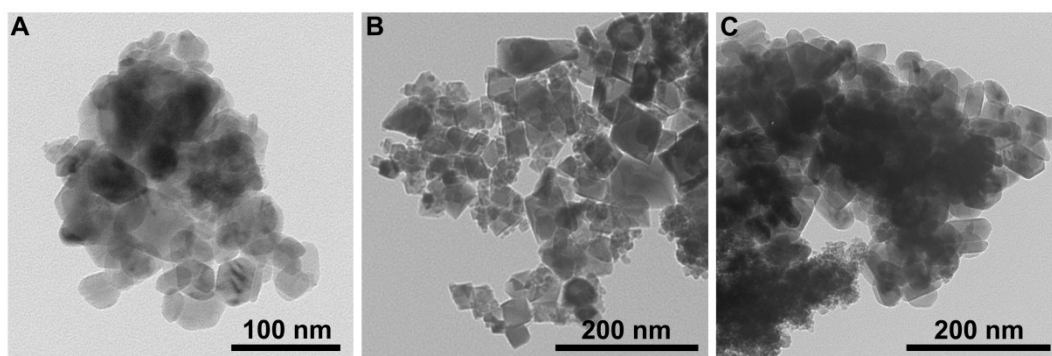


Fig. S5 TEM images of the nanoparticles detached from the B-Fe/B-NiCo, HT-NiCoFe and B-Fe, respectively.

Table S1. ICP results of the catalysts.

	Ni (%)	Co (%)	Fe (%)
B-NiCoFe (Co:Ni=1:1)	24.3	22.3	53.4
B-Fe/B-NiCo	52.1	47.9	-
HT-NiCoFe	42.5	40.3	17.2
B-Fe	-	-	100
B-NiCoFe (Co:Ni=2:1)	12.6	30.1	57.3
B-NiCoFe (Co:Ni=1:2)	34.0	12.8	53.2

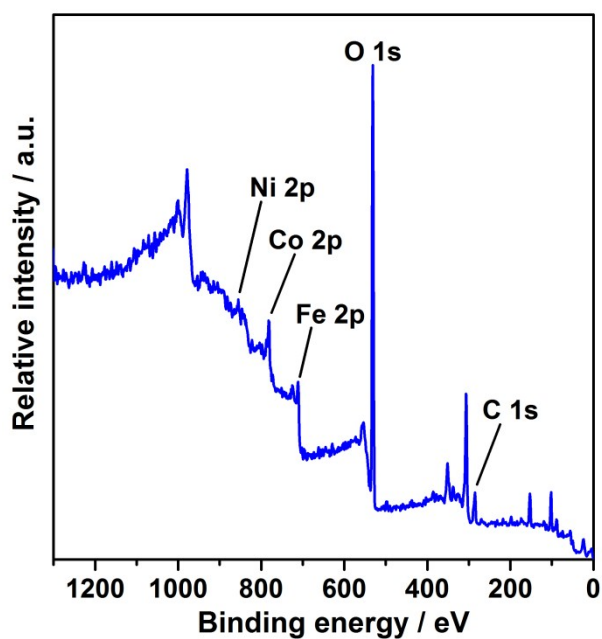


Fig. S6 XPS survey spectra of the B-NiCoFe.

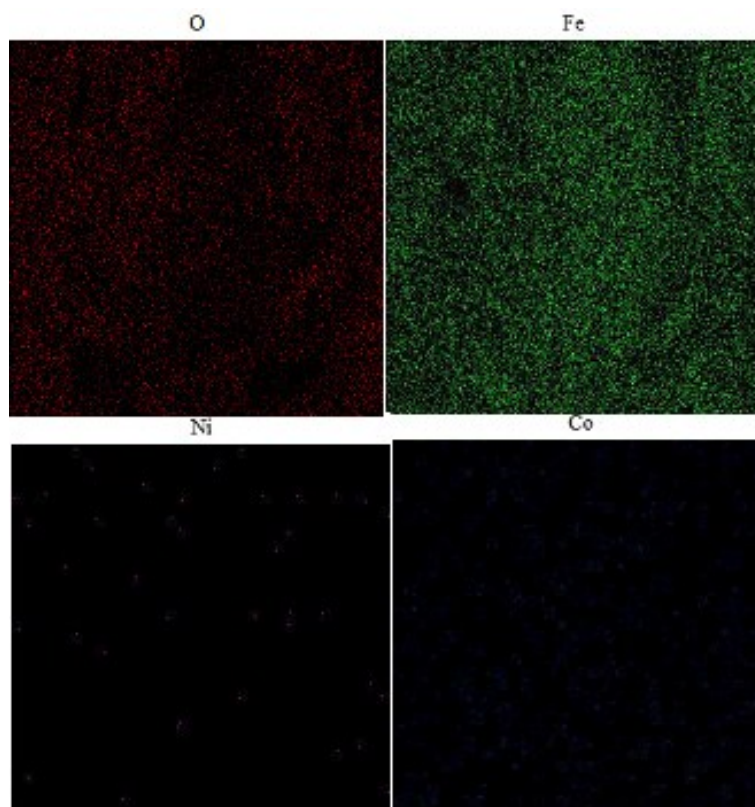


Fig. S7 EDX elemental mapping analyses of the B-NiCoFe catalyst confirm the homogeneous distribution of O, Fe, Ni and Co and the dominance of Fe, which is consistent with the ICP result.

The estimation of the electrochemically active surface area of the samples was carried out according to literature.^[1-2] CV measurements were taken in the region of 1.0-1.1 V vs. RHE without redox reactions at various scan rates (20, 40, 60, 80, 100 mV s⁻¹, etc.), which are mainly considered as the double-layer capacitive behavior. The electrochemical double-layer capacitance (C_{dl}) of various catalysts can be determined from the CV plots, which is expected to be linearly proportional to the effective surface area. The double-layer capacitance is estimated by plotting the Δj ($j_a - j_c$) at 1.05 V vs. RHE against the scan rate, where the slope is twice C_{dl} . The calculated C_{dl} values are listed in Table S2.

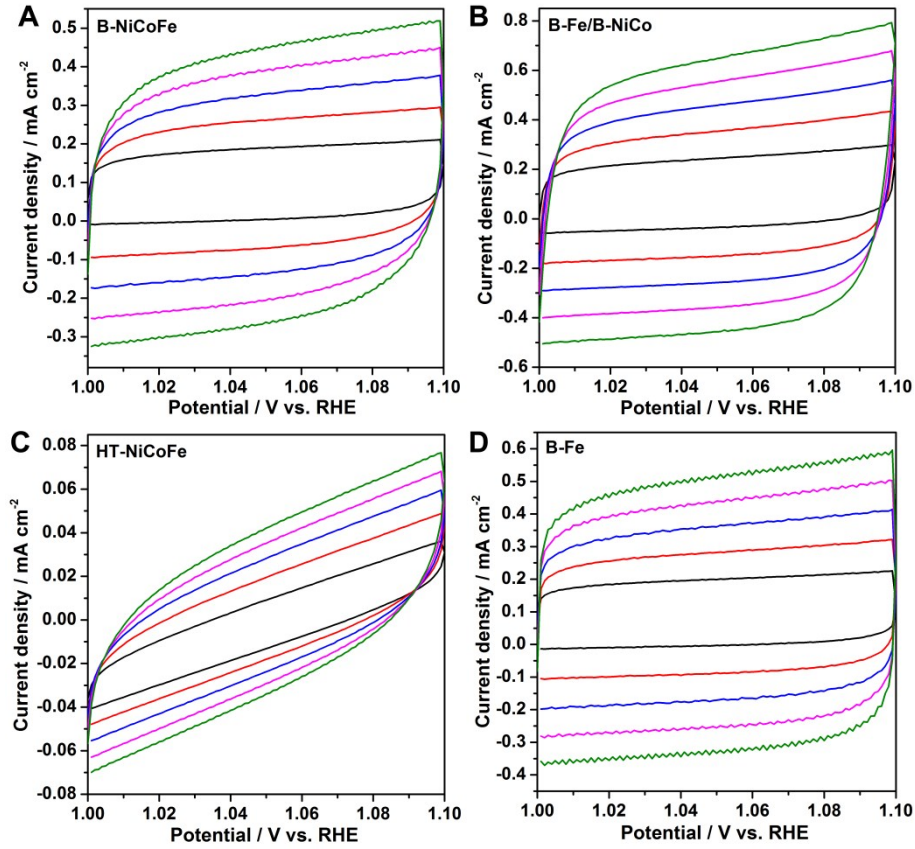


Fig. S8 CV curves in the non-redox region for the estimation of C_{dl} .

Table S2. Comparison of the electrochemical parameters in OER catalysis.

	R_s [Ω]	R_{ct} [Ω]	C_{dl} [mF cm^{-2}]	η_{10mA} cm^{-2} [mV]	j_{geo} @ $\eta=500$ mV [mA cm^{-2}]	Tafel slope [mV dec^{-1}]	j_{cat} @ $\eta=400$ mV [A F^{-1}]
B-NiCoFe	3.3	39	5.74	342	110.5	48	6.0
B-Fe/B-NiCo	4.5	272	5.14	396	78.8	82	2.2
HT-NiCoFe	5.4	172 4	0.40	-	2.0	142	2.5
B-Fe	6.0	374	4.01	388	72.5	80	3.5

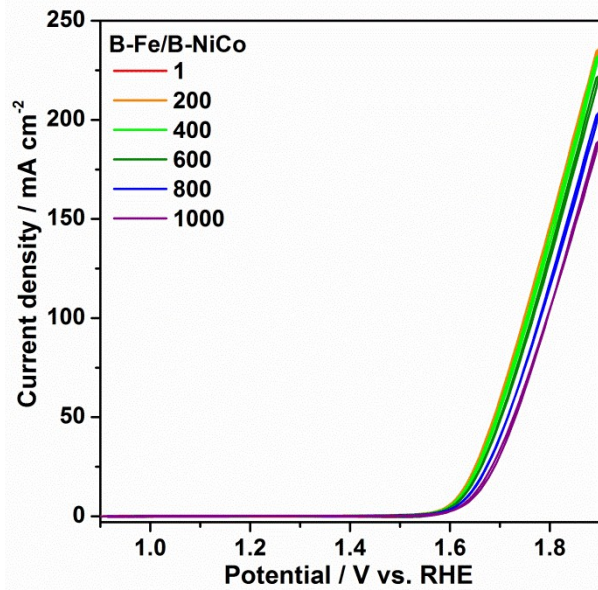


Fig. S9 Potential cycling test of the B-Fe/B-NiCo catalyst.

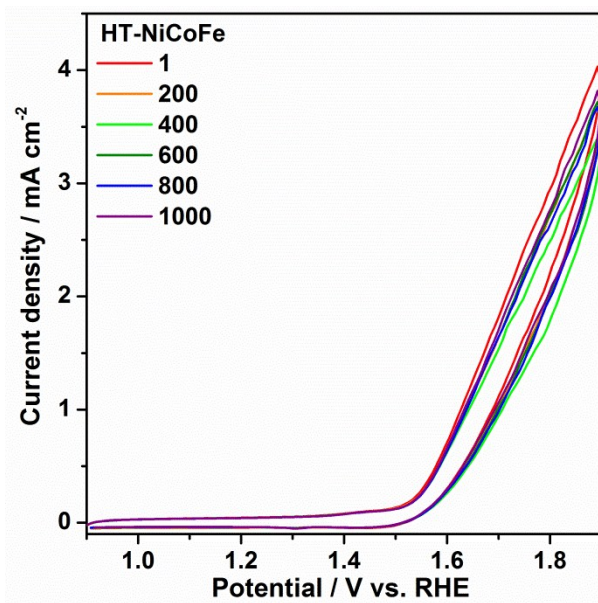


Fig. S10 Potential cycling test of the HT-NiCoFe catalyst.

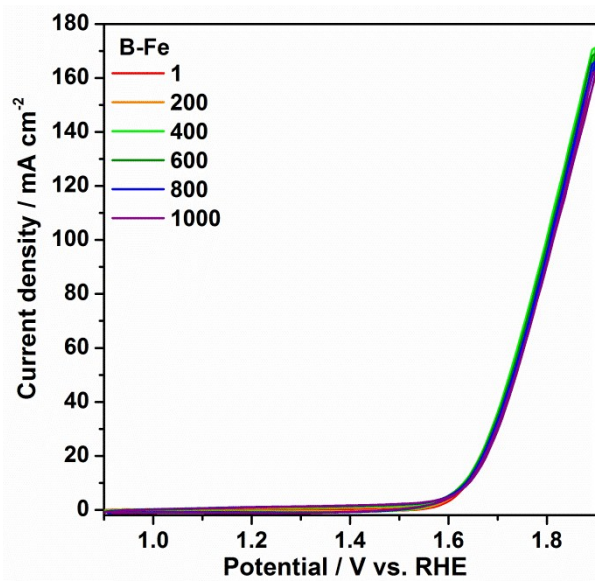


Fig. S11 Potential cycling test of the B-Fe catalyst.

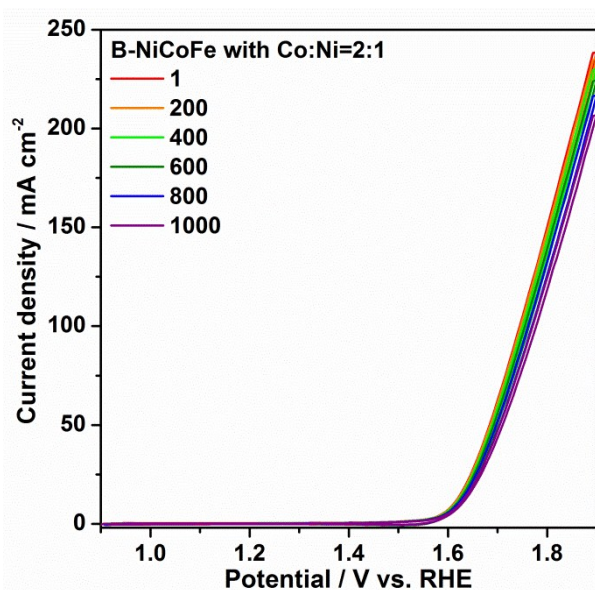


Fig. S12 Potential cycling test of the B-NiCoFe catalyst with Co:Ni ratio of 2:1.

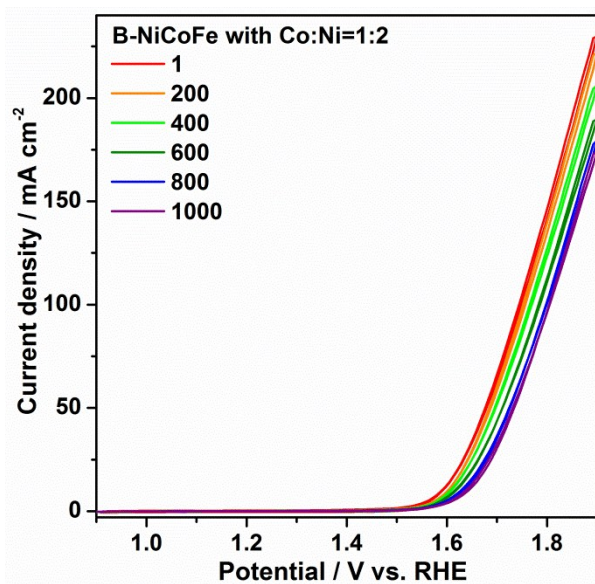


Fig. S13 Potential cycling test of the B-NiCoFe catalyst with Co:Ni ratio of 1:2.

Reference

- [1] M. A. Lukowski, A. S. Daniel, F. Meng, A. Forticaux, L. Li, S. Jin, *J. Am. Chem. Soc.* **2013**, *135*, 10274-10277.
- [2] J. Xie, J. Zhang, S. Li, F. Grote, X. Zhang, H. Zhang, R. Wang, Y. Lei, B. Pan and Y. Xie, *J. Am. Chem. Soc.* **2013**, *135*, 17881-17888.